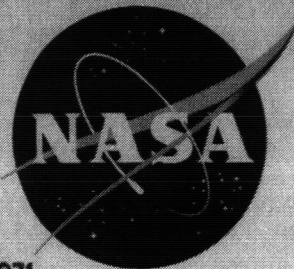


NASA TM X-602

CLASSIFICATION CHANGED
UNCLASSIFIEDTO
By Authority of 21-617 Date 5 OCT 1971

TECHNICAL MEMORANDUM

X-602 Declassified by authority of NASA
Classification Change Notices No. 215
Dated 21 DEC 1971STATIC LONGITUDINAL AERODYNAMIC CHARACTERISTICS OF A MODEL
OF A TWO-STAGE VERSION OF A SATURN LAUNCH VEHICLEWITH A PROPOSED APOLLO PAYLOAD AT
MACH NUMBERS FROM 1.57 TO 2.87

By James R. Morgan and Roger H. Fournier

Langley Research Center
Langley Air Force Base, Va.NATIONAL AERONAUTICS AND SPACE ADMINISTRATION
WASHINGTON

September 1961

W

DECLASSIFIED

NATIONAL AERONAUTICS AND SPACE ADMINISTRATION

TECHNICAL MEMORANDUM X-602

STATIC LONGITUDINAL AERODYNAMIC CHARACTERISTICS OF A MODEL

OF A TWO-STAGE VERSION OF A SATURN LAUNCH VEHICLE

WITH A PROPOSED APOLLO PAYLOAD AT

MACH NUMBERS FROM 1.57 TO 2.87*

By James R. Morgan and Roger H. Fournier

SUMMARY

The static longitudinal aerodynamic characteristics of a model of a two-stage version of a Saturn launch vehicle with a possible Apollo payload shape were investigated in the Langley Unitary Plan wind tunnel. The effects of an escape tower attached to the payload and two arrangements of octaform fins attached to the rear section of the first stage were determined. The investigation was conducted over a Mach number range from 1.57 to 2.87 and an angle-of-attack range from about -8° to 8° .

The results of this investigation indicate that the addition of an escape tower to the model (with four large cruciform fins and four stub cruciform fins interdigitated with the large fins and attached to the base of the model) causes abrupt changes in the slope of the pitching-moment curves. Replacing the four large cruciform fins with four stub fins (resulting in an octaform stub-fin arrangement) shifts the center of pressure forward about 1.46 model diameters.

INTRODUCTION

Wind-tunnel investigations are being conducted by the National Aeronautics and Space Administration to determine the static longitudinal aerodynamic characteristics of Saturn launch vehicles. As part of this program, tests have been made at supersonic speeds on a model of a two-stage version of a Saturn launch vehicle with a proposed Apollo payload shape with two octaform fin arrangements at the base of the model. In one configuration, the fin arrangements contain four large stabilizing

*Title, Unclassified.

cruciform fins with four stub cruciform fins interdigitated with the large fins; and in the second configuration, the fin arrangement was an octaform grouping of stub fins. In addition, the effects of an escape tower, similar to that used in Project Mercury, attached to the Apollo payload shape were determined for the combination of large and stub fins in octaform arrangement.

This investigation was conducted in the Langley Unitary Plan wind tunnel at Mach numbers from 1.57 to 2.87 over an angle-of-attack range from about -8° to 8° .

Transonic results for a similar model are presented in reference 1.

COEFFICIENTS AND SYMBOLS

The data of this investigation are presented about the system of axes shown in figure 1. Moment coefficients are referred to a point located on the model center line at 9.176 inches from the base of the model. This moment center corresponds to the full-scale center-of-gravity location during flight over a Mach number range from about 2.9 to 3.5. The coefficients and symbols are defined as follows:

C_A	axial-force coefficient, $\frac{\text{Axial force}}{qS}$
$C_{A_{\alpha=0}}$	axial-force coefficient at $\alpha = 0^\circ$
C_m	pitching-moment coefficient, $\frac{\text{Pitching moment}}{qSd}$
C_{m_α}	slope of pitching-moment coefficient curve at $\alpha = 0^\circ$, $\frac{\partial C_m}{\partial \alpha}$, per degree
C_N	normal-force coefficient, $\frac{\text{Normal force}}{qS}$
C_{N_α}	slope of normal-force coefficient curve at $\alpha = 0^\circ$, $\frac{\partial C_N}{\partial \alpha}$, per degree
d	reference diameter (diameter of a circle which would enclose first-stage tanks), 4.130 inches
M	Mach number

q	free-stream dynamic pressure, 0.7 pM^2 , lb/sq ft
S	reference area (cross-sectional area of circle which would enclose first-stage tanks), 0.0929 sq ft
$\frac{x_{cp}}{d}$	location of center of pressure in body diameters from moment center (positive values are upstream of moment center)
α	angle of attack of model center line, deg
R	Reynolds number
r	radius
p	free-stream static pressure, lb/sq ft
p_t	free-stream stagnation pressure, lb/sq in.
X,Y,Z	coordinate axes

MODEL AND APPARATUS

The model consisted of a two-stage version of a Saturn launch vehicle with a proposed Apollo payload and two octaform fin arrangements at the base of the model. (See fig. 2(a).) An escape tower, similar to that of Project Mercury, was attached to the Apollo by three rods which formed, in cross section, an equilateral triangle. The base of the triangle was in the horizontal plane (fig. 2(b)) and on the lower side of the model. The fin arrangements contained a combination of four large stabilizing cruciform fins and four stub cruciform fins interdigitated with the large fins and an octaform arrangement of stub fins. (Fin details are shown in fig. 2(c).) The model was oriented so that the pitch and yaw planes coincided with the large fins. Photographs of the models are presented in figure 3.

The tests were conducted in the low Mach number test section of the Langley Unitary Plan wind tunnel. This tunnel is a variable-pressure, continuous, return-flow type with a test section 4 feet square and approximately 7 feet in length. An asymmetric sliding block nozzle provides a means to vary the Mach number continuously from 1.57 to 2.87.

Forces and moments acting on the model were measured by an internal strain-gage balance. The model support system consisted of a balance-model-sting combination attached to a remotely operated adjustable angle

0317130A 1030

03

4

coupling connected to the tunnel central support system. Pressure measurements at the base of the model were made with a pressure-sensitive electrical pickup.

TESTS

The model configurations tested include the two-stage Saturn launch vehicle, four-large- and four-stub-fin arrangement and the Apollo payload with and without escape tower. Also the two-stage launch vehicle, Apollo payload with escape tower, and an eight-stub-fin arrangement was tested. All model configurations were tested through an angle-of-attack range from about -8° to 8° at an angle of sideslip of 0° at Mach numbers of 1.57, 1.80, 2.16, and 2.87. Test conditions are summarized in the following table:

M	p_t , lb/sq in.	q , lb/sq ft	R/ft
1.57	10.0	611	2.70×10^6
1.80	12.0	682	3.00
2.16	14.7	688	3.14
2.87	22.5	619	3.15

Transition was fixed on the nose of the model by means of a 1/8-inch-wide band of 0.009-inch-diameter roughness particles. The method used to determine the roughness height is presented in reference 2. Roughness particles of 0.005 inch were determined from this method but, by visual inspection of shadowgraphs during progress of the test, the 0.005-inch transition particles did not appear to produce a turbulent boundary layer at the transition location. Therefore, the particle size was increased to 0.009 inch and this size particle appeared to produce transition. Location of the transition strip is shown in figure 2(a).

CORRECTIONS AND ACCURACIES

All angles of attack have been adjusted for flow angularity and structural deflection of the sting-balance combination under load. Axial-force coefficients have been adjusted to correspond to free-stream static pressure acting at the base of the model. The maximum deviation of the local Mach number in the region of the tunnel occupied by the model is ± 0.015 . The estimated accuracies of the angle of attack and the coefficients, based on balance calibration and repeatability of the



DECLASSIFIED

5

data, are within the following limits:

α , deg	± 0.1
C_N	± 0.026
C_m	± 0.021
C_A	± 0.005

PRESENTATION OF RESULTS

The results of this investigation are presented in the following figures:

	Figure
Schlieren photographs	4
Longitudinal characteristics:	
Model with large and stub fins, escape tower off	5
Model with large and stub fins, escape tower on	6
Model with stub fins only, escape tower on	7
Summary of the longitudinal characteristics	8

DISCUSSION

The results of this investigation are presented herein without analysis. However, some observations were made on the results and are discussed briefly.

In general, the variation of the pitching moment with angle of attack is nonlinear for all model configurations tested. (See figs. 5 to 7.) Addition of the escape tower to the model causes abrupt changes in the slope of the pitching-moment curves (compare figs. 5 and 6) and shifts the center of pressure rearward about 0.35 model diameters at $M = 1.57$. Flow separation over and immediately back of the tower probably causes the slope changes in the pitching-moment characteristics.

It should be noted that the apparent stabilizing effect of the escape tower occurs over a small angle-of-attack range near 0° and does not affect the stability characteristics at the higher angles of attack. The normal-force characteristics were unaffected by the escape tower; however, the axial-force coefficients are reduced throughout the Mach number range. (See fig. 8.) This reduction in axial force is a result of the weaker bow compression coming from the escape tower, whereas, a much stronger bow compression exists without the tower.

031712281030

8

The model configurations with the large and stub fin arrangement are stable for the test moment-center location and Mach numbers. The test moment-center location is somewhat (about 0.11d) forward of the center-of-gravity location for flight at the test Mach numbers. Consequently, the flight stability level of these configurations would be reduced from those presented herein, and a near-neutral stability level would result at the higher Mach numbers. Although there are many conditions which must be considered in determining the acceptable level of stability, one of the more critical is structural loading. From this viewpoint, a configuration of low stability would not experience the structural problems of a configuration having large stability or large instability.

Replacing the four large cruciform fins with four stub cruciform fins (resulting in an octaform stub-fin arrangement) shifts the center of pressure forward by as much as 1.46 model diameters at $M = 1.57$ and 0.66 diameter at $M = 2.87$ (fig. 8); therefore, an unstable configuration results.

CONCLUDING REMARKS

The results of wind-tunnel tests of a model of a two-stage version of a Saturn launch vehicle with a proposed Apollo payload and two octaform fin arrangements over a Mach number range from 1.57 to 2.87 indicate that the addition of an escape tower to the configuration with four large stabilizing cruciform fins and four stub cruciform fins, interdigitated with the large fins, causes abrupt changes in the slope of the pitching-moment curves. Replacing the four large cruciform fins with four stub cruciform fins, resulting in an octaform stub-fin arrangement, shifts the center of pressure forward as much as 1.46 model diameters.

Langley Research Center,
National Aeronautics and Space Administration,
Langley Air Force Base, Va., August 2, 1961.



DECLASSIFIED

REFERENCES

1. Pearson, Albin O.: Wind-Tunnel Investigation at Mach Numbers From 0.30 to 1.20 of the Static Aerodynamic Characteristics of a Two-Stage Saturn Launch Vehicle. NASA TM X-601, 1961.
2. Braslow, Albert L., and Knox, Eugene C.: Simplified Method for Determination of Critical Height of Distributed Roughness Particles for Boundary-Layer Transition at Mach Numbers From 0 to 5. NACA TN 4363, 1958.

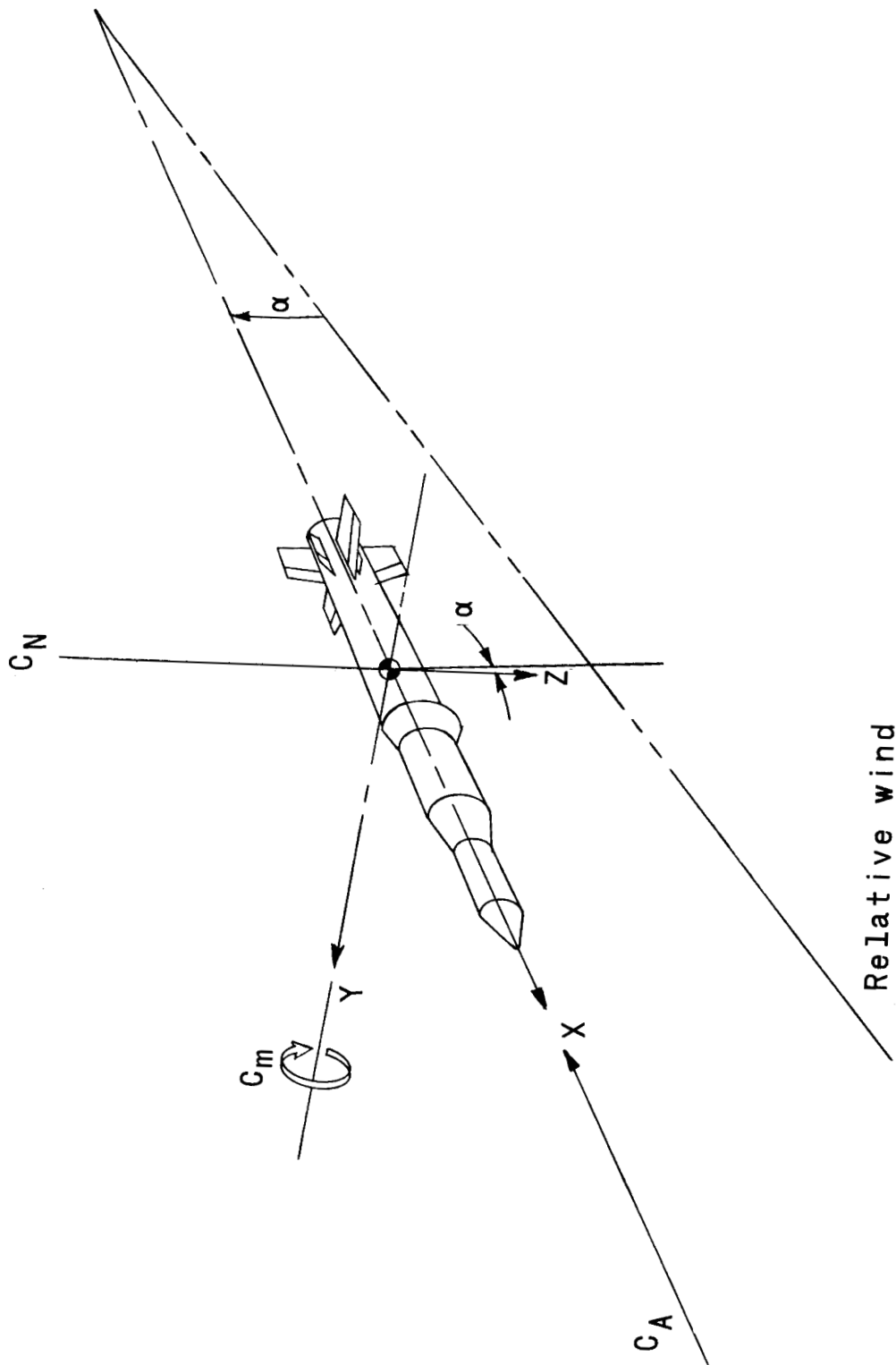
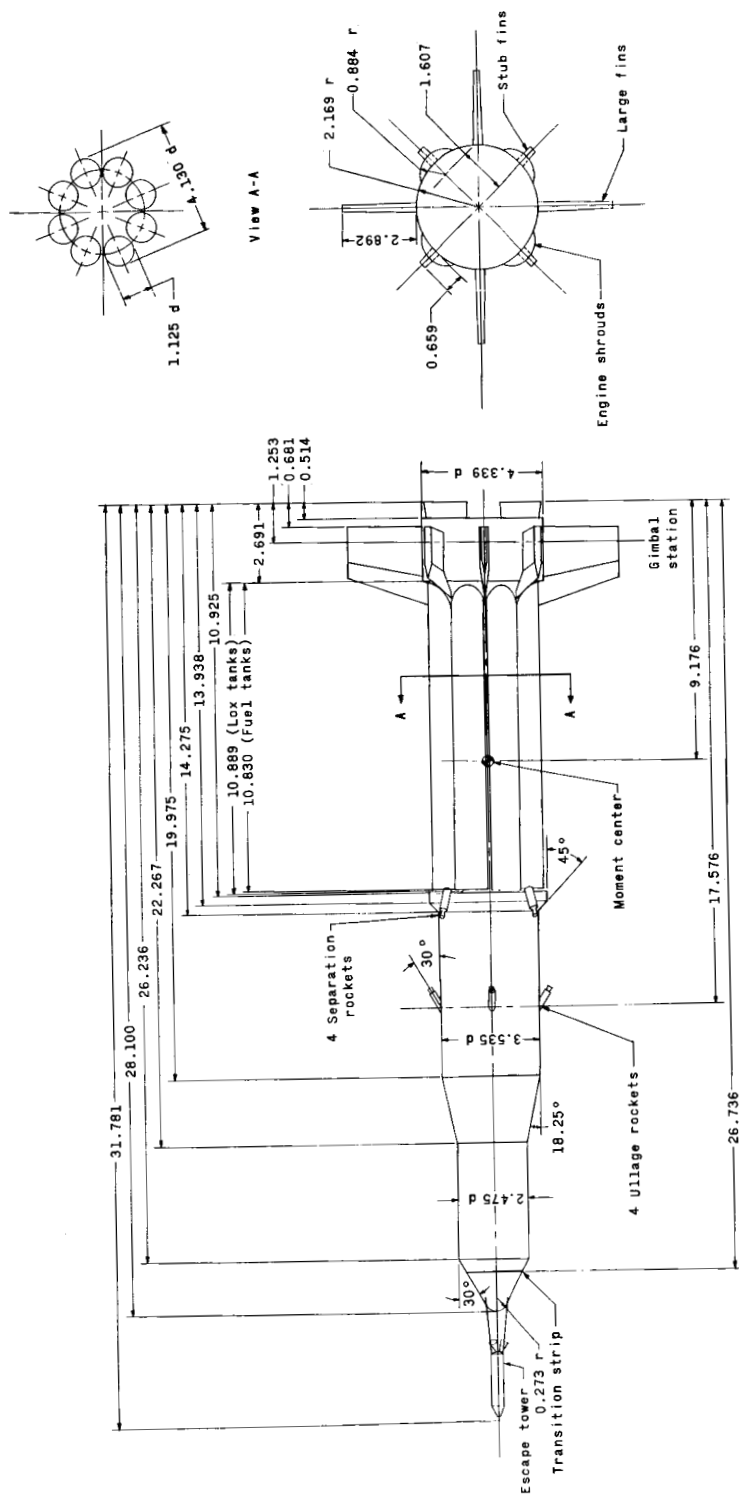


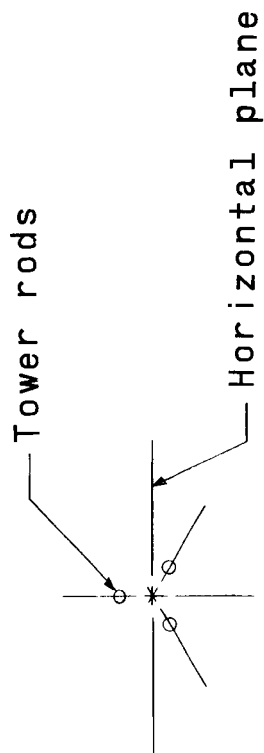
Figure 1.- System of axes. Arrows indicate positive values.



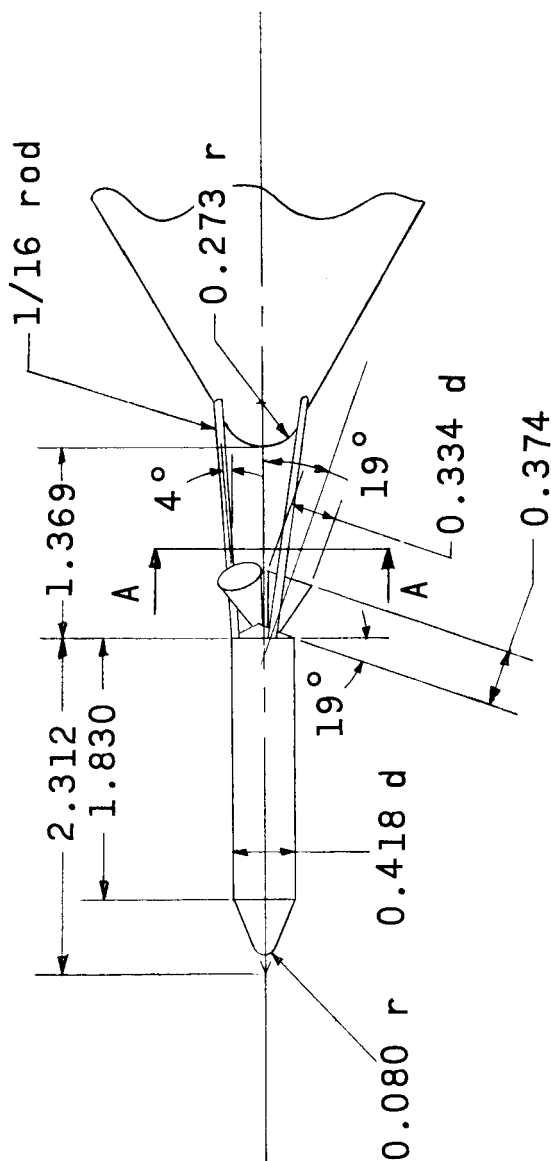
(a) Two-stage version of the Saturn launch vehicle with proposed Apollo payload and octaform fin arrangement.

Figure 2.- Details of the model tested. All dimensions are in inches unless otherwise specified.

0374238538

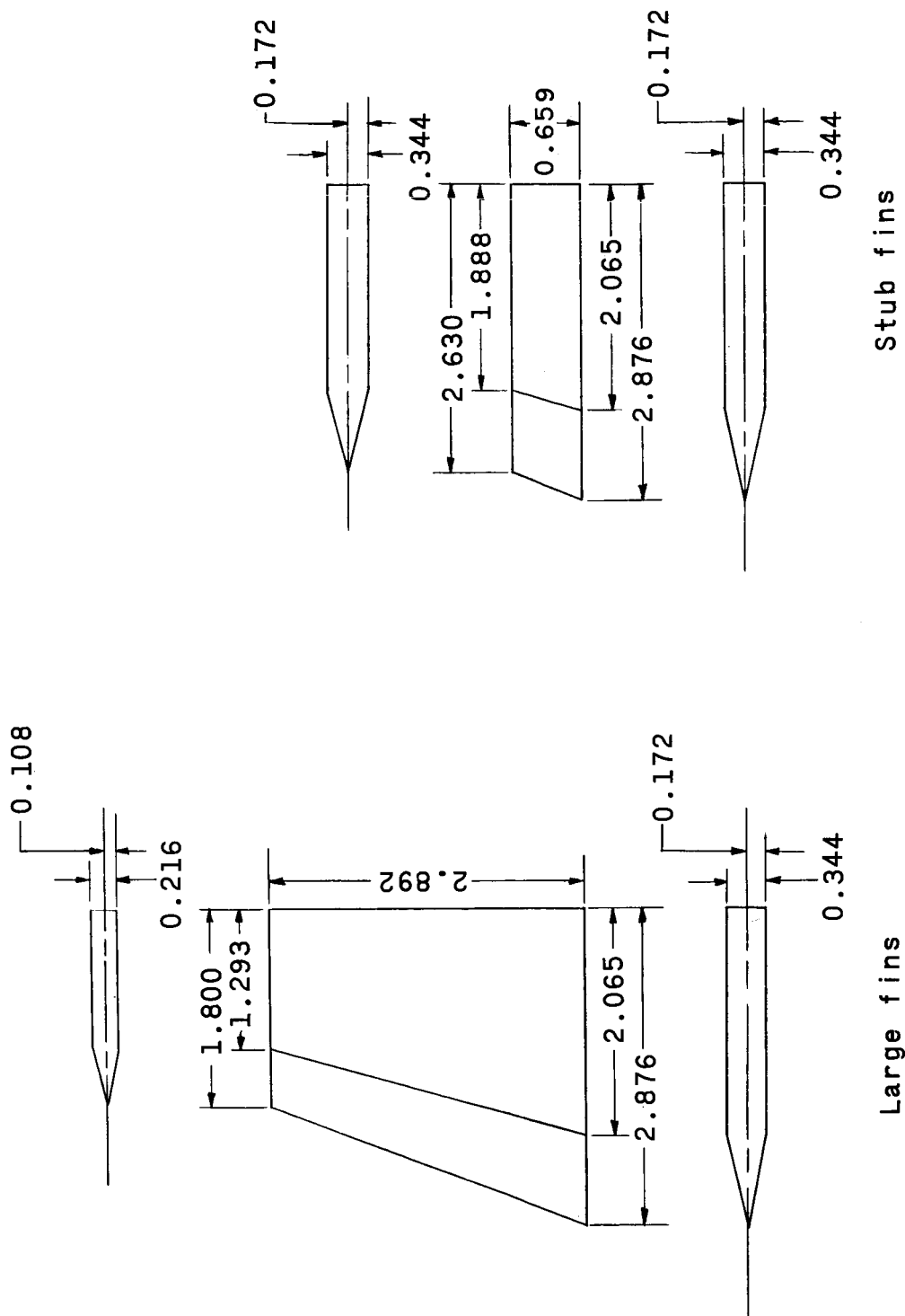


View A-A



(b) Detail of the escape tower.

Figure 2.- Continued.

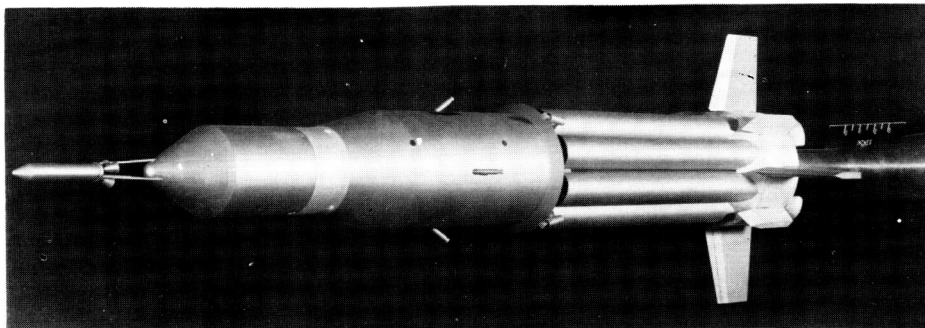


(c) Detail of fins.

Figure 2.- Concluded.

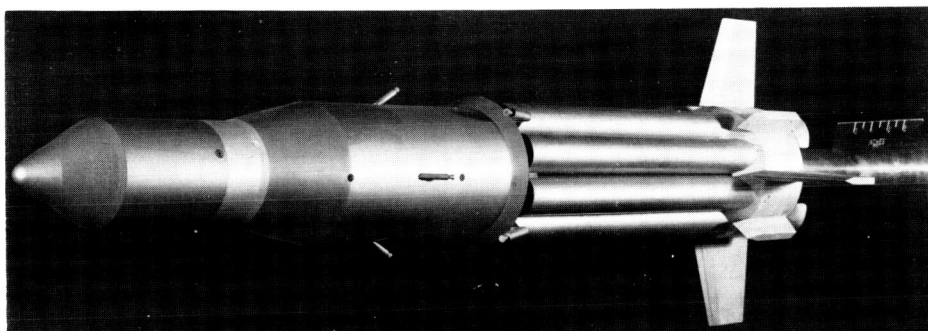
0371020.1031

8



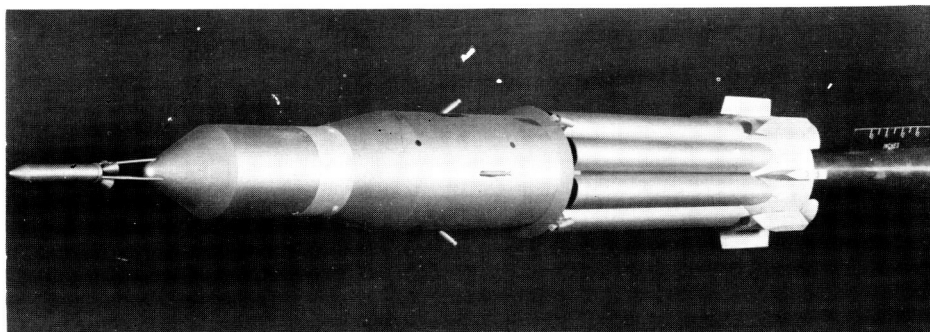
Escape tower on; 4 large
and 4 stub fins

L-61-4793



Escape tower off; 4 large
and 4 stub fins

L-61-4797



Escape tower on;
8 stub fins

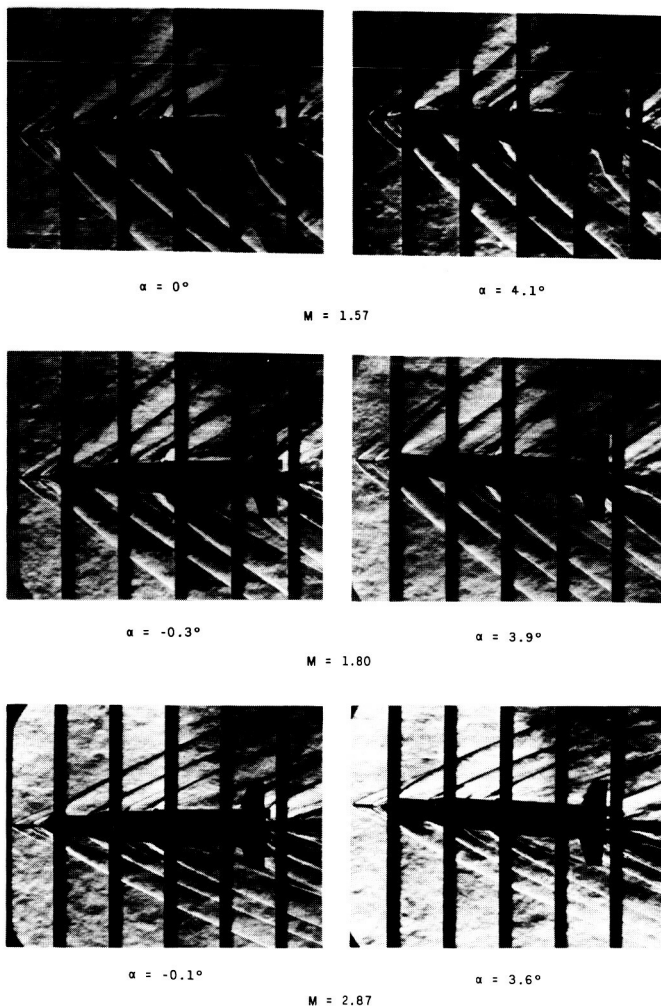
Figure 3.- Photographs of the models tested.

L-61-4792



DECLASSIFIED

13

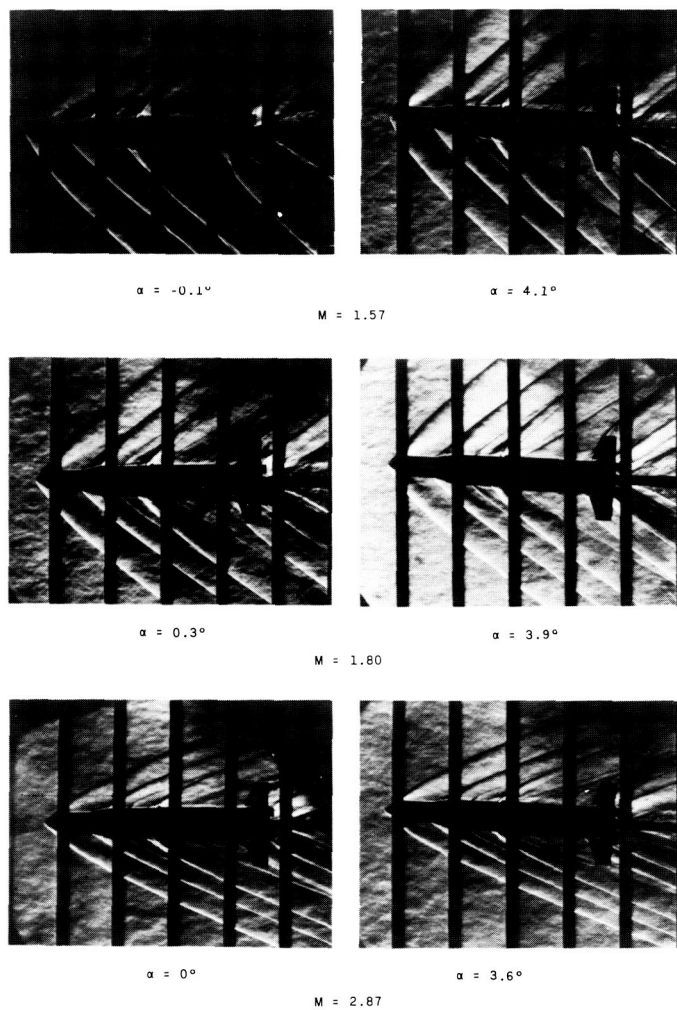


(a) Escape tower on.

L-61-5054

Figure 4.- Schlieren photographs of the model with and without escape tower.

031712201030



(b) Escape tower off.

L-61-5055

Figure 4.- Concluded.

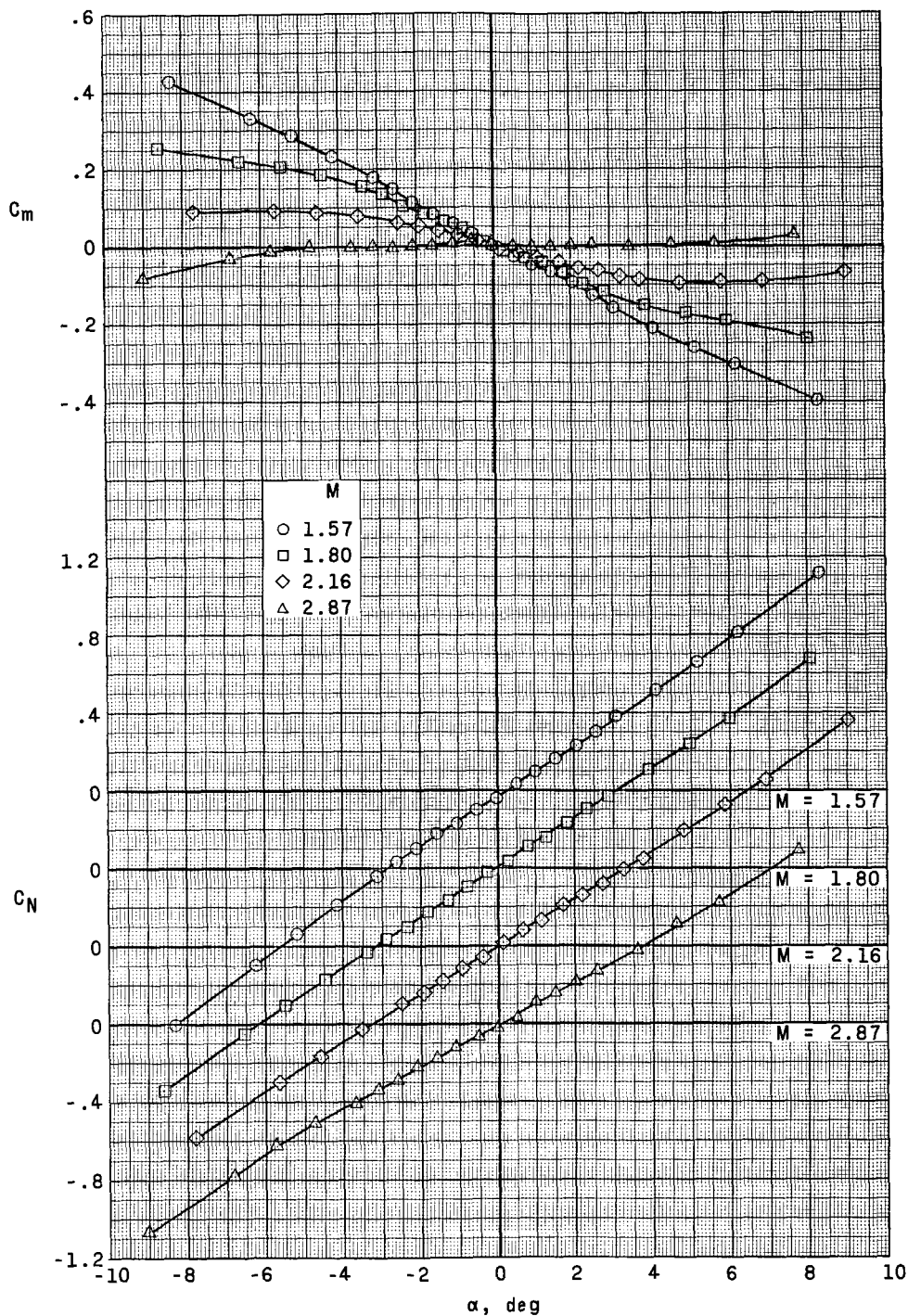


Figure 5.- Aerodynamic characteristics in pitch of the model without escape tower and four large and four stub fins.

037039 039

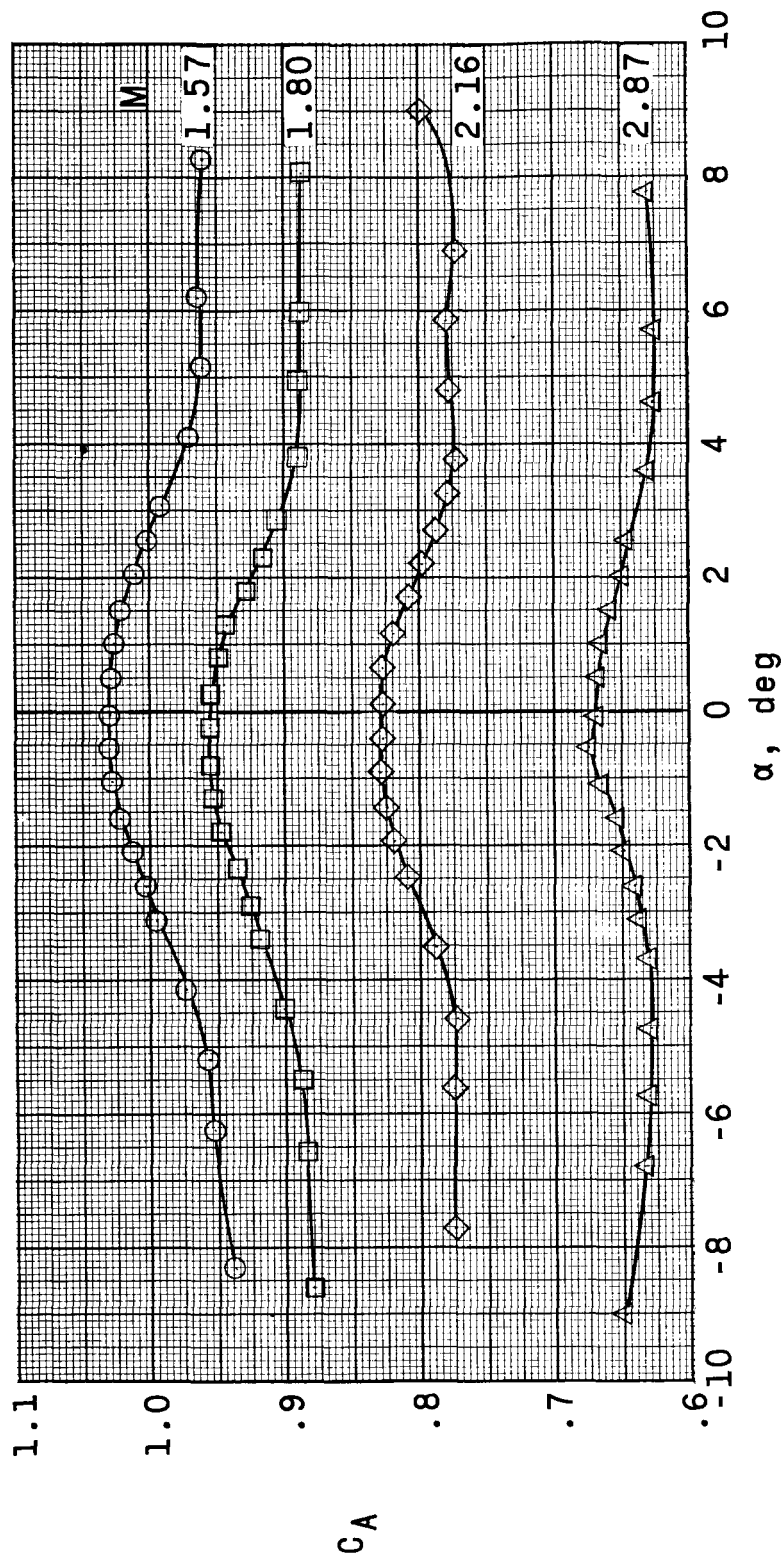


Figure 5.- Concluded.

Figure 1 consists of two vertically stacked graphs sharing a common x-axis representing the angle of attack α in degrees, ranging from -10 to 10. The top graph plots the coefficient of the velocity potential C_m on the y-axis, ranging from -0.4 to 0.6. It shows four data series for Mach numbers $M = 1.57$ (circles), $M = 1.80$ (squares), $M = 2.16$ (diamonds), and $M = 2.87$ (triangles). All series show a decreasing trend as α increases, with a sharp drop around $\alpha = 0$. The bottom graph plots the lift coefficient C_N on the y-axis, ranging from -1.2 to 1.2. It shows the same four data series for $M = 1.57, 1.80, 2.16, 2.87$. The lift coefficient increases linearly with α for negative angles and then deviates from linearity for positive angles, with the deviation becoming more pronounced at higher Mach numbers.

Figure 6.- Aerodynamic characteristics in pitch of the model with escape tower and four large and four stub fins.

03903 133

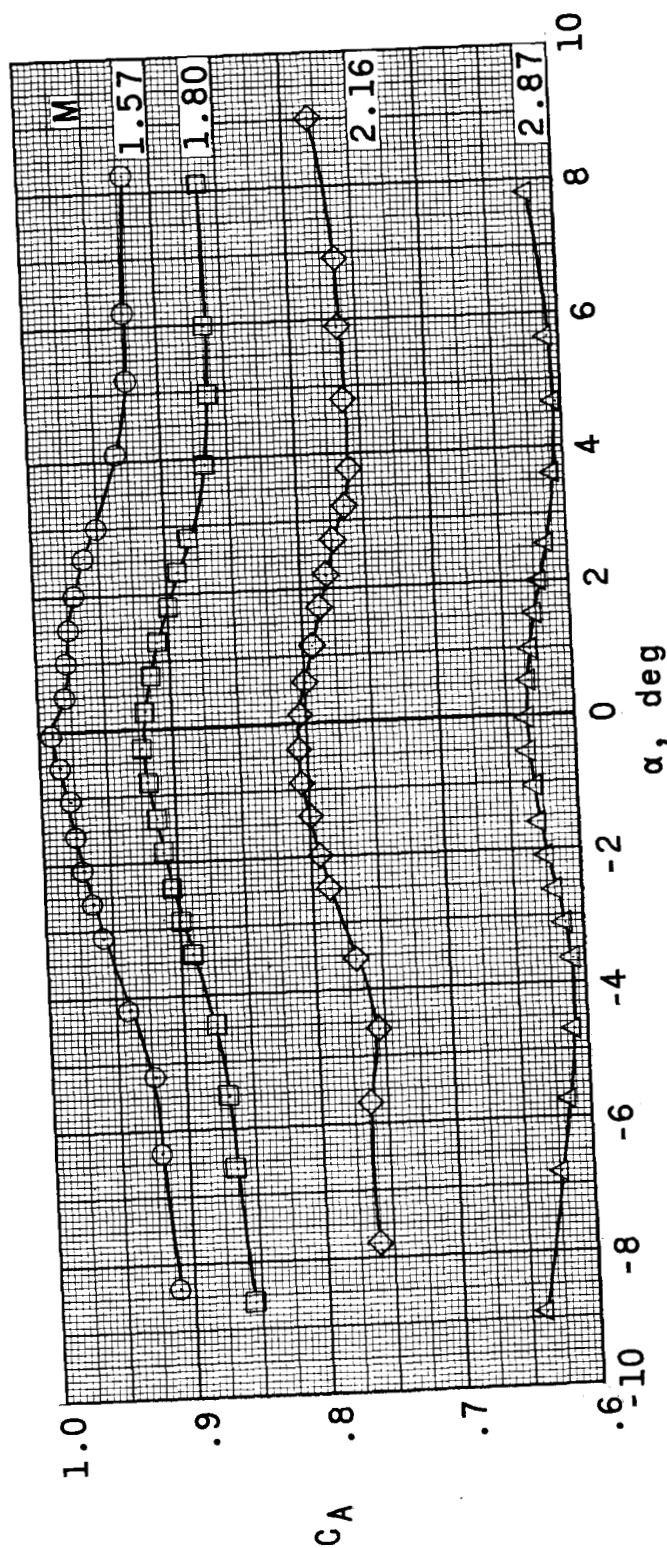


Figure 6.- Concluded.



DECLASSIFIED

19

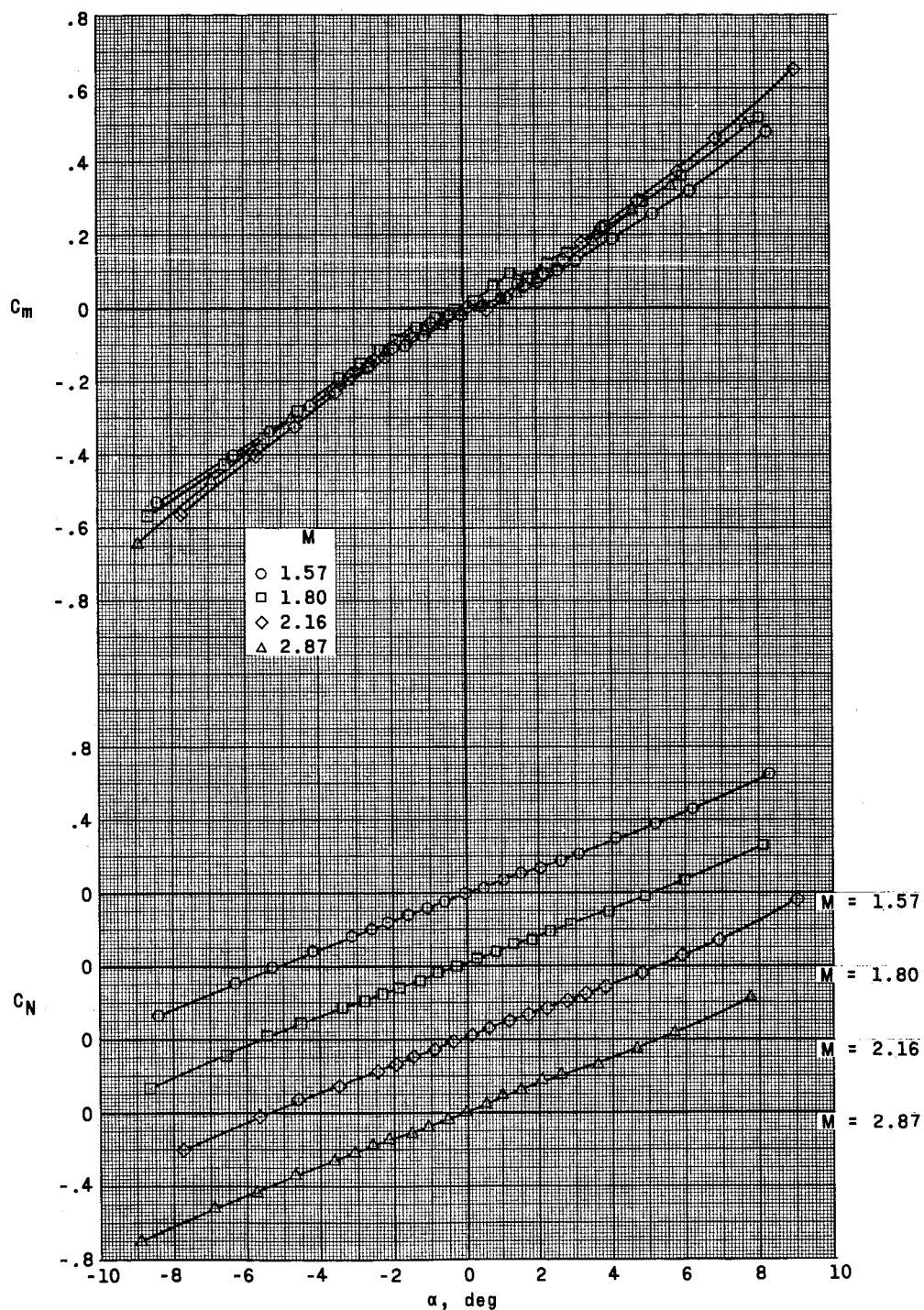


Figure 7.- Aerodynamic characteristics in pitch of the model with escape tower and eight stub fins.

037036 133

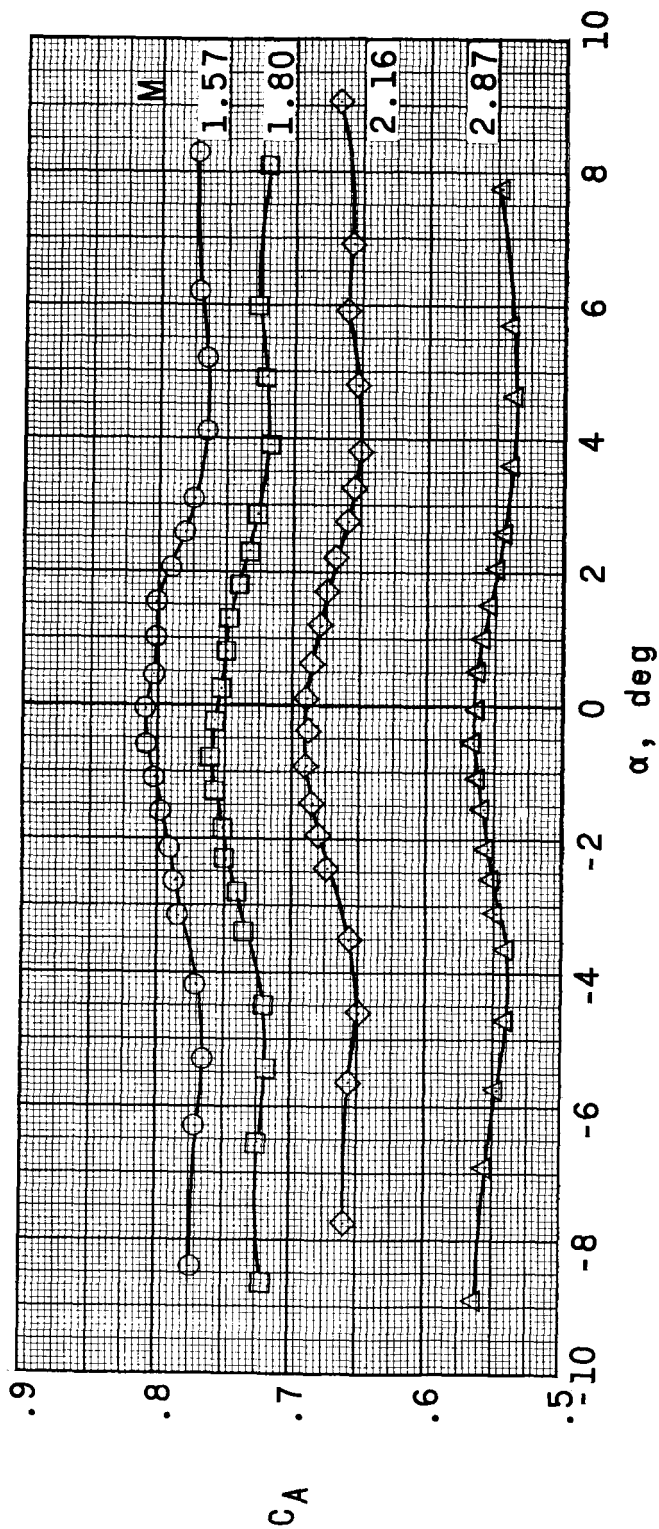


Figure 7.- Concluded.



DECLASSIFIED

21

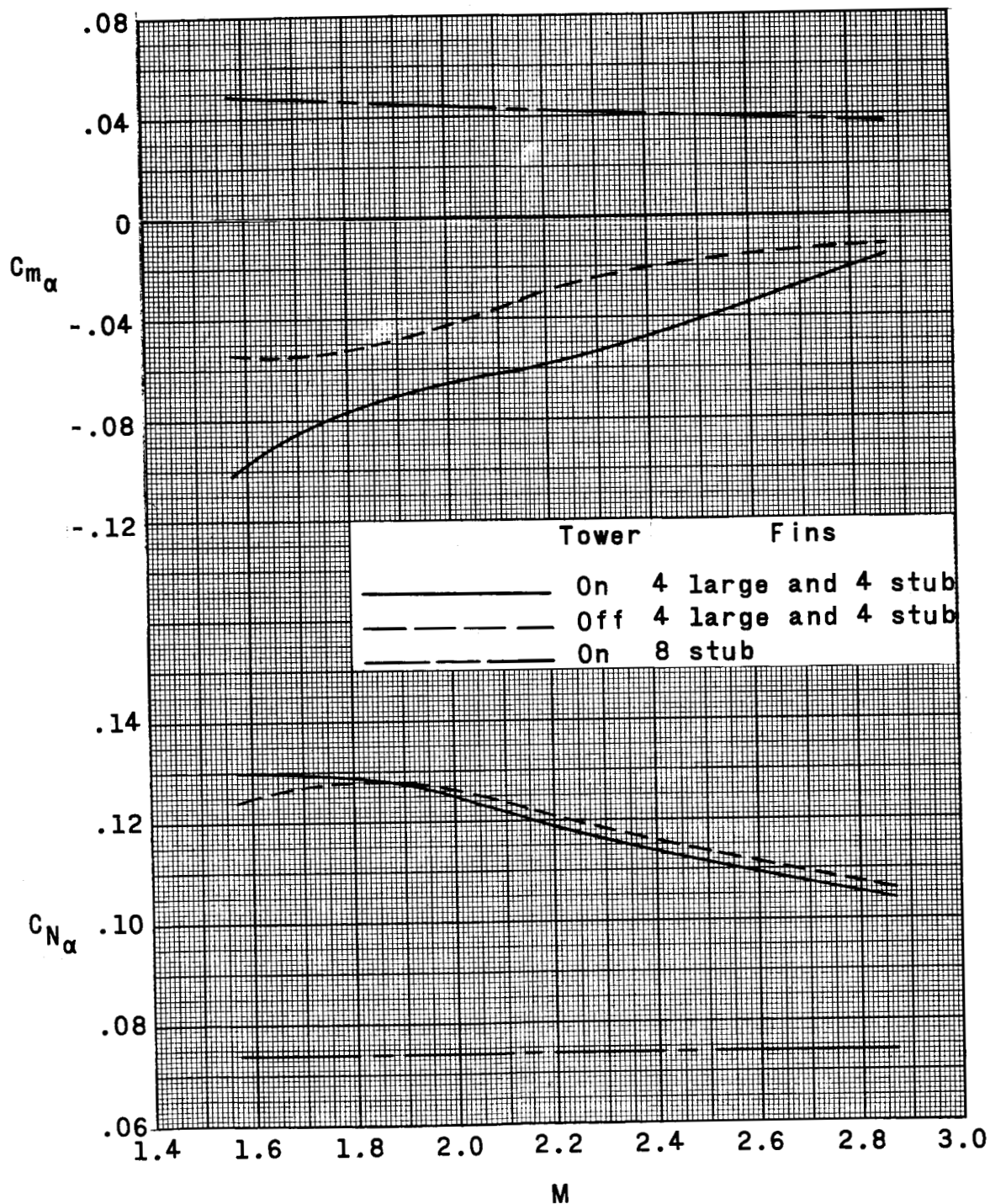


Figure 8.- Summary of the aerodynamic characteristics in pitch of all model configurations tested.

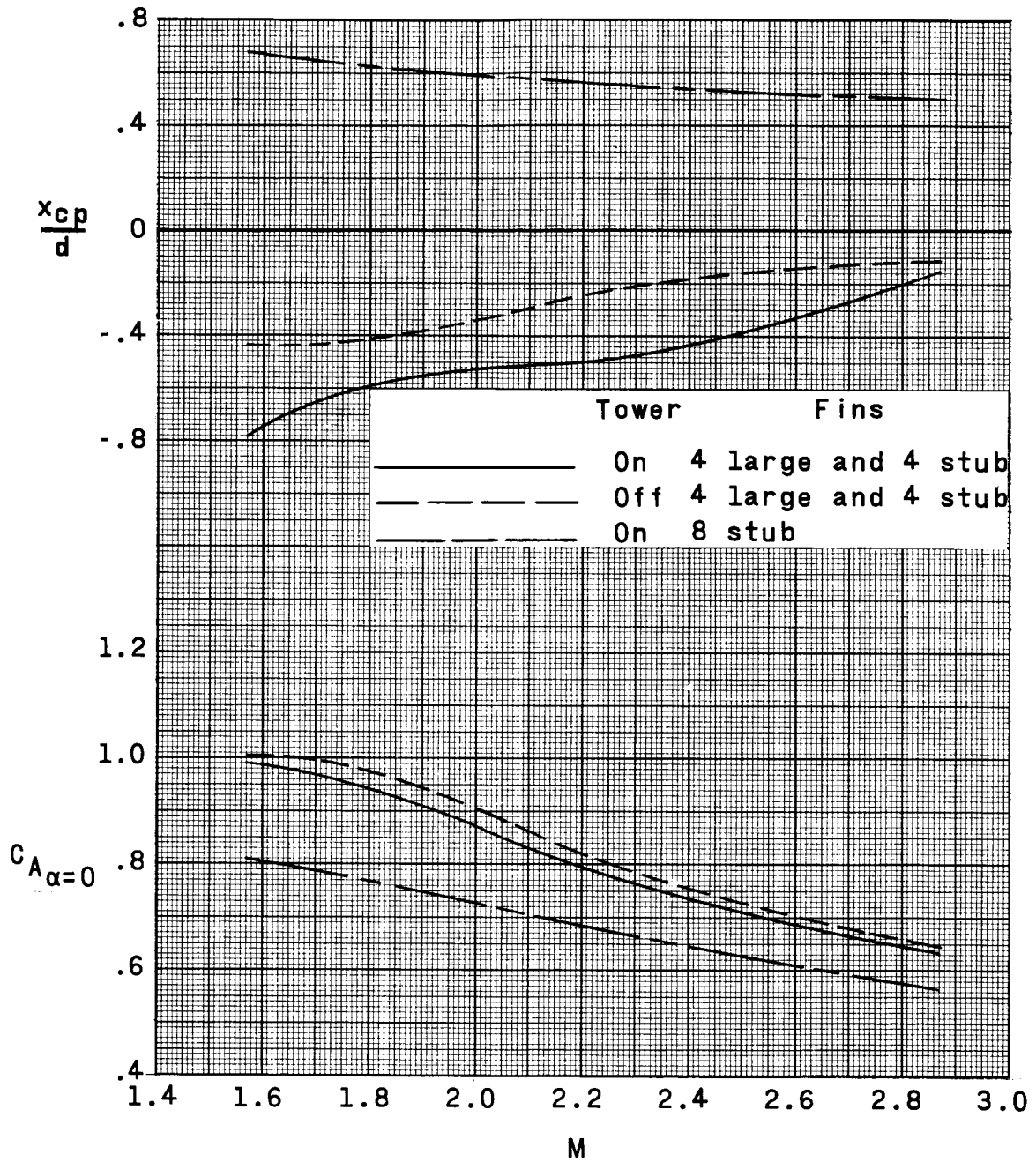


Figure 8.- Concluded.